



Published in final edited form as:

Angew Chem Int Ed Engl. 2016 July 25; 55(31): 8923–8927. doi:10.1002/anie.201603149.

Demonstrating Uranium as a Visible Light Photocatalyst For C_{sp^3} -H Fluorination**

Julian G. West, T. Aaron Bedell, and Erik J. Sorensen*

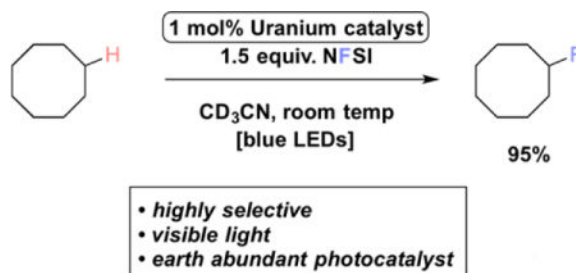
Department of Chemistry, Princeton University, Princeton, NJ

Abstract

The fluorination of unactivated C_{sp^3} -H bonds remains a desirable, challenging transformation for pharmaceutical, agricultural, and materials scientists. Previous methods for this transformation have used bench-stable fluorine atom sources; however, many still rely on the use of UV-active photocatalysts for the requisite high-energy hydrogen atom abstraction event. Herein, we describe the use of uranyl nitrate hexahydrate as a convenient, hydrogen atom abstraction catalyst that can mediate fluorinations of certain alkanes upon activation with visible light.

Graphical abstract

U can do it: Uranyl cation (UO_2^{2+}) is able to effect the catalytic fluorination of unactivated C_{sp^3} -H bonds under visible light irradiation. This report highlights uranyl nitrate as a convenient, molecular C-H abstraction catalyst that exhibits selectivity distinct from previously reported catalytic systems.



Keywords

Uranium; photocatalysis; hydrogen atom transfer; C-H activation; fluorination

Fluorine has gained a privileged position in the fields of medicinal,¹ agricultural,² and materials chemistry³ for the desirable characteristics that it can confer on the constituent matter of each field. Isosteric (but certainly not electronically similar) with hydrogen, the

**This work was supported by NIGMS R01 GM065483 to E.J.S., NSF-GRFP DGE 1148900 to J.G.W., the NSF-CCI Center for Selective C-H Functionalization (CHE-1205646), and Princeton University.

*ejs@princeton.edu.

This paper is dedicated with respect and admiration to Prof. Martin F. Semmelhack on the occasion of his 75th birthday.

Supporting information for this article is given via a link at the end of the document.

fluorine atom permits modulation of myriad molecular properties, including partitioning behavior, acidity of neighboring groups, and metabolic stability.⁴ Fluorine incorporation has traditionally been achieved through use of pre-fluorinated building blocks, limiting the possible sources of fluorine to commercially available compounds. Even deoxyfluorination, one of the more robust techniques for the targeted incorporation of fluorine, requires the pre-existence of oxygenated functionality. For this reason, direct, late-stage fluorinations of unactivated C_{sp3}-H bonds presents an enticing platform for accessing compounds beyond the confines of fine chemicals catalogues.⁵

While the fluorination of C_{sp3}-H bonds using elemental fluorine has been common since the Second World War,⁶ the low selectivity of this transformation, combined with the operationally non-trivial nature of handling elemental fluorine, has fueled the recent interest⁵ in selective C_{sp3}-H fluorination using safe, bench stable reagents. Indeed, the recent reports from Lectka,⁷ Britton,⁸ Chen,⁹ and Tan¹⁰ suggests that, despite progress, this transformation is not yet a solved problem. With some exceptions,^{11,12,13} recent strategies for selectively fluorinating C_{sp3}-H bonds have largely recruited photo-hydrogen atom abstraction (HAT) catalysts (denoted [cat]), such as acetophenone, anthraquinone, 1,2,4,5-tetracyanobenzene, and tetra-*n*-butylammonium decatungstate (TBADT, Figure 1), to generate a carbon-centered radical. This radical can react with a fluorine atom source (R_nN-F), typically the electrophilic N-F fluorination reagents *N*-fluorobenzenesulfonimide (NFSI, Figure 1) or Selectfluor (figure 1), in a mode first recognized by Sammis,¹⁴ to furnish the desired product. These processes are rendered catalytic through the oxidizing nature of the generated aminyl radical (denoted R_nN•) (NFSI) or radical cation (Selectfluor), which can return the photoreduced HAT catalyst to its initial state. These methods, while enabling, share one drawback: the need for ultraviolet (UV, or hν 200–400 nm) irradiation. While not all UV photoreactions require specialized equipment, many use low efficiency light sources and can induce side reactions. Therefore, it would be desirable to modulate the light requirement of the photo-HAT catalyst into the visible (hν 400–750 nm) range.¹⁵ Toward realizing this aim, we sought a HAT catalyst that could be activated with low energy light.

Uranium is an element that has become inextricably linked to the applications of its fissile isotope, ²³⁵U, toward power generation and nuclear weaponry. Surprisingly, 99.3% of natural uranium is made up of the non-fissile isotope ²³⁸U, a species whose main application is filling storage bins near enrichment facilities after removal of ²³⁵U (approximately 95% of all depleted uranium produced to date is stored this way).¹⁶ The removal of ²³⁵U makes handling depleted uranium no more arduous than that of other heavy metals.¹⁷ This depleted uranium represents a substantial untapped resource, as its crustal abundance exceeds that of molybdenum,¹⁸ an element common enough to be used as an enzymatic cofactor. Indeed, despite this glut of depleted uranium, much of its fundamental, structural chemistry is only recently coming to light,¹⁹ with its applications in catalysis lagging even further behind.^{20,21}

One aspect of uranium chemistry that has been well studied, however, is the photochemistry of the uranyl cation (UO₂²⁺).^{22–24} Studies by multiple groups have revealed several intriguing characteristics, notably that a highly-oxidizing excited state, [UO₂]^{2+*} (+2.6 V vs SHE, almost equal to the oxidizing power of elemental fluorine!²⁵) is accessible under blue light (hν 450–495 nm) irradiation. This excited state is sufficiently reactive to abstract

hydrogen atoms from unactivated (BDE > 100 kcal/mol) C–H bonds to generate carbon-centered radicals. Furthermore, pioneering studies by Bakac and coworkers showed that this reactivity could be rendered catalytic for aerobic oxidation of alkanes (Figure 2); with some substrates, the quantum yield approaches unity.^{26,27} Despite this promising reactivity and abundance of desirable characteristics, the applications of the uranyl cation in catalysis remain largely underdeveloped.

Based on this known photochemistry and initial report of catalytic activity, we hypothesized that the uranyl cation would be an ideal photo-HAT catalyst for the fluorination of unactivated C_{sp3}–H bonds via the mechanism outlined in Figure 1. Putting this supposition to the test, we subjected cyclooctane, NFSI, and 1 mol% uranyl acetate dihydrate to blue LED irradiation to form fluorocyclooctane in a modest, catalytic 8% yield (Entry 1, Table 1). Replacing the uranyl source with uranyl nitrate hexahydrate, led to a greatly improved yield of 52%, corresponding to 52 turnovers (Entry 2, Table 1). Use of a higher intensity blue light source further improved the reaction efficiency, with the near quantitative formation of fluorocyclooctane possible after 16 hours of irradiation (>95%/>95 turnovers, Entry 3, Table 1), exceeding the efficiencies of the acetophenone⁹ and 1,2,4,5-tetracyanobenzene⁷ methods (yields of 82%/16 turnovers and 62%/6.2 turnovers, respectively). Both light and catalyst are required for the reaction, and reduction of the NFSI loading below 1.5 equivalents or the uranyl nitrate loading below 1 mol% reduced the efficiency (Table 1, Entries 4–7). Finally, acetone could be substituted as the reaction solvent with comparable efficiencies (Table 1, Entry 8).

With a rapid, efficient, visible light-mediated fluorination method in hand, we turned our attention to probing the substrate scope of the reaction. Initial testing found that cyclohexane and cyclopentane exhibited diminished, yet still moderate efficiencies at 42% and 32% yields, respectively (Table 2, Entries 2 and 3). The cause of this lower progress is currently unknown; however, a similar (though less pronounced) reduction in efficiency compared to cyclooctane was observed for the fluorination of cyclohexane using both the acetophenone⁹ and 1,2,4,5-tetracyanobenzene⁷ systems (yields of 59%/12 turnovers and 45%/4.5 turnovers, respectively). *n*-Alkanes provided a mixture of fluorinated products at methylene positions (Table 2, Entries 4 and 5).

A fluorinated motif that occupies a privileged place in the fields of medicinal and agricultural chemistry is the trifluoromethyl²⁸ functionality. Toward producing this functionality, toluene was subjected to the reaction conditions to furnish benzyl fluoride in trace yields, corresponding to a minimal consumption of starting material and NFSI; 4-cyanotoluene behaved similarly (Table 2, Entries 6 and 7).

Having achieved validation of the method on hydrocarbon substrates, our interests turned to the reaction of related oxygenates. Acetone, the simplest aliphatic ketone, displayed no detectable reactivity under our reaction conditions (Table 3, Entry 1). Increasing the chain length of the ketone substrate led to the production of some fluorinated products in trace yields (Table 3, Entries 2–4), with residual mass balance being unreacted starting material; cyclopentanone (Table 3, Entry 5) was similarly inert. As with ketones, esters were resistant to fluorination for short chain lengths (Table 3, Entries 6–8), but became suitable substrates

as chain length increased, providing distal, internal functionalization (Table 3, Entry 9). Interestingly, ethyl isovalerate (Table 3, Entry 10) performed significantly better than its linear counterpart (Table 3, Entry 8), with the more complex natural product sclareolide performing yet better, furnishing 26% of the combined α - and β -fluorinated products (Table 3, Entry 11). While it appears that proximity to carbonyl functionalities is highly deactivating for the fluorination reaction, the low reactivity of carbonyl-containing substrates cannot be explained by electronic effects alone.

These results from carbonyl-containing substrates are in sharp contrast to those of previously reported photo-HAT fluorination methods, where high reactivity is observed despite sensitivity to electronic effects. An example is sclareolide: acetophenone⁹ (80%/16 turnovers), anthraquinone¹⁰ (77%/39 turnovers), 1,2,4,5-tetracyanobenzene⁷ (61%/6.1 turnovers), and TBADT⁸ (68%/34 turnovers) all produced mixtures of monofluorinated products in moderate to high yields as compared to the low result observed for the uranium system (26%/26 turnovers, Table 3, Entry 11). Similarly, acetal and ether functional groups are incompatible with the uranyl system, with the dioxolane derived from condensing cyclopentanone with ethylene glycol providing even less reactivity than the parent ketone (Table 3, Entry 12) and *tert*-butyl methyl ether not producing any fluorinated product. (Table 3, Entry 13). Taken together, the presence of a Lewis-basic oxygen site on the substrate, even the traditionally weak coordinator carbonyl, appears to be deleterious to the reaction.

An initial hypothesis combining these two observations posits that carbonyls might be quenching the uranyl excited state via a reversible, inner-sphere electron transfer. Indeed, it is known that ketones will readily coordinate the labile $[\text{UO}_2]^{2+}$ cation, with such intermediates having been observed experimentally.²⁹ Bakac and coworkers²⁷ previously observed this non-productive quenching via “exciplex decay” in the aerobic oxidation of toluene, finding that the vast majority of interactions between toluene and the uranyl excited state, $[\text{UO}_2]^{2+*}$, led to return to the ground-state with no HAT (figure 3). We encountered this same phenomenon when attempting to fluorinate toluene and, to an even greater extent, anisole, a substrate that would have been interesting as a model for the production of agrochemically valuable mono-, di-, and tri-fluoromethoxy³⁰ ethers (Table 3, Entry 14).

Compelling evidence for the exciplex decay of the arene substrates comes from a competitive quenching experiment, wherein an equimolar amount of toluene and cyclooctane was subjected to the fluorination and quantified. The low yields of both products (Figure 4) suggest that this is at least partially responsible for the low efficiency. Returning to the question of ketones, an analogous experiment using equimolar cyclopentanone and cyclooctane led to high yield of fluorocyclooctane (74%, Figure 4) and trace fluorinated cyclopentanone, suggesting that cyclopentanone is at best a weak quencher of the uranyl excited state, $[\text{UO}_2]^{2+*}$. If one imagines a slow, but competitive with HAT, intramolecular deactivation pathway for carbonyl compounds, the improved activity of ethyl isovalerate, long chain esters and sclareolide compared to cyclopentanone could be explained through several factors. These might include additional activation, and thus higher rate of reaction, of a methine proton (ethyl isovalerate); a greater number of potential reactive sites (longer chain substrates); and structural rigidity separating the reactive site from a potential quenching functionality (sclareolide).

Regardless of cause, the limited substrate scope of the uranyl fluorination, while initially disheartening, is not without benefits. Firstly, the (essentially) complete inertness of short-chain ketones and relative unreactivity of other carbonyl compounds contrasts with the TBADT⁸- and acetophenone⁹-mediated reactions, for which they are excellent substrates. In the substrate admixing experiments of Figure 4, the selective activation of cyclooctane (BDE 96 kcal•mol⁻¹)³² over toluene (BDE 90 kcal•mol⁻¹)³³ is interesting and again diverges greatly from arylketone^{9,34}- and TBADT³⁵-catalyzed fluorination methods, wherein benzylic positions are preferentially activated. This highly-discriminating nature of the uranyl catalyst opens the door for selective fluorination of electronically activated C–H bonds in the presence of others that would be a liability under previously-reported conditions.

A second upside to this observation is the contribution of a new data point to the sparsely populated chart of uranyl photocatalysis. The benchmarking of this promising complex against popular photo-HAT catalysts in an increasingly well-studied reaction class shows that while many comparisons can be made, so can many contrasts. The behavior of cyclooctane shows that the efficiency of uranyl photocatalysis can outstrip that of traditional near-UV photo-HAT catalysts while operating under visible light; however, the substrate must be chosen judiciously.

Ultimately, a new catalytic method to fluorinate certain unactivated C_{sp3}–H bonds was developed; this method uses low-energy visible light to drive homolytic cleavages of strong C–H bonds by an activated uranyl catalyst and capitalizes on the reactivity of a putative organic radical. To the best of our knowledge, this chemistry constitutes the second catalytic transformation based on the HAT reactivity of a photo-activated uranyl catalyst. Our hope is that the research described herein will stimulate future efforts to expand the considerable potential of abundant, yet underutilized, uranyl complexes in catalysis.

Supplementary Material

Refer to Web version on PubMed Central for supplementary material.

References

1. Kirk KL. *Org Process Res Dev.* 2008; 12:305–321.
2. Fujiwara T, O'Hagan D. *J Fluorine Chem.* 2014; 167:16–29.
3. Berger R, Resnati G, Metrangolo P, Weber E, Hulliger J. *Chem Soc Rev.* 2011; 40:3496–3508. [PubMed: 21448484]
4. Hagmann WG. *J Med Chem.* 2008; 51:4359–4369. [PubMed: 18570365]
5. Neumann CN, Ritter T. *Angew Chem Int Ed.* 2015; 54:3216–3221.
6. McBee ET. *Ind Eng Chem.* 1947; 39:236–237.
7. Blum S, Knippel JL, Lectka T. *Chem Sci.* 2014; 5:1175–1178.
8. Halperin SD, Fan H, Chang S, Martin RE, Britton R. *Angew Chem Int Ed.* 2014; 53:4690–4693.
9. Xia JB, Zhu C, Chen C. *Chem Commun.* 2014; 50:11701–11704.
10. Kee CW, Chin KF, Wong MW, Tan CH. *Chem Commun.* 2014; 50:8211–8214.
11. Chambers RD, Parsons M, Sanford G, Bowryden R. *Chem Commun.* 2000:959–960.
12. Liu W, Huang MJ, Nielsen RJ, Goddard W, Groves JT. *Science.* 2012; 337:1322–1325. [PubMed: 22984066]

13. Blum S, Pitts CR, Miller DC, Haselton N, Holl MG, Urheim E, Lectka T. *Angew Chem Int Ed*. 2012; 51:10580–10583.
14. Rueda-Becerril M, Sazepin CC, Leung JCT, Okbinoglu T, Kennepohl P, Paquin JF, Sammis GM. *J Am Chem Soc*. 2012; 134:4026–4029. [PubMed: 22320293]
15. Prier CK, Rankic DA, MacMillan DWC. *Chem Rev*. 2013; 113:5322–5363. [PubMed: 23509883]
16. Hubbell, MW. *The Fundamentals of Nuclear Power Generation: Questions and Answers*. Author House; Bloomington: 2011.
17. Princeton University. “Uranium and Thorium Use”, can be found under. 2015. <https://ehs.princeton.edu/laboratory-research/radiation-safety/radioactive-materials/uranium-thorium-use>
18. Lide, D. *CRC Handbook of Chemistry and Physics, 2000–2001*. CRC Press; Boca Raton: 2000.
19. Little ST. *Angew Chem Int Ed*. 2015; 54:8604–8641.
20. Fox AR, Bart SC, Meyer K, Cummins CC. *Nature*. 2008; 455:341–349. [PubMed: 18800133]
21. Li Y, Su J, Mitchell E, Zhang G, Li J. *Sci China Chem*. 2013; 56:1671–1681.
22. Burrows HD, Kemp TJ. *Chem Soc Rev*. 1974; 3:139–165.
23. Syt’ko VV, Umreiko DS. *J Appl Spectrosc*. 1998; 65:857–870.
24. Paine, RT.; Kite, MS. *Lanthanide and Actinide Chemistry and Spectroscopy*. American Chemical Society; Washington D.C.: 2009. p. 369-380.
25. Jørgensen CK, Reisfield R. *Struct Bond*. 1982; 50:121–171.
26. Wang WD, Bakac A, Espensen JH. *Inorg Chem*. 1995; 34:6034–6039.
27. Mao Y, Bakac A. *J Phys Chem*. 1996; 100:4219–4223.
28. Barata-Vallejo S, Lantaño B, Postigo A. *Chem Eur J*. 2014; 51:16806–16829.
29. Rios D, Schoendorff G, Van Stipdonk MJ, Gordon MS, Windus TL, Gibson JK, de Jong WA. *Inorg Chem*. 2012; 51:12768–12775. [PubMed: 23146003]
30. Leroux FR, Manteax B, Vors JP, Pazenok S. *Beilstein J Org Chem*. 2008; 4:13. [PubMed: 18941485]
31. Matsushima K. *J Am Chem Soc*. 1972; 94:6010–6016.
32. Periyar A, Bose S, Biswas AN, Barman S, Bandyopadhyay P. *Catal Sci Technol*. 2014; 4:3180–3185.
33. Nam PC, Nguyen MT. *J Phys Chem A*. 2005; 109:10342–10347. [PubMed: 16833329]
34. Xia JB, Zhu C, Chen C. *J Am Chem Soc*. 2013; 135:17494–17500. [PubMed: 24180320]
35. Nodwell MB, Bagai A, Halperin SD, Martin RE, Knust H, Britton R. *Chem Commun*. 2015; 51:11783–11786.

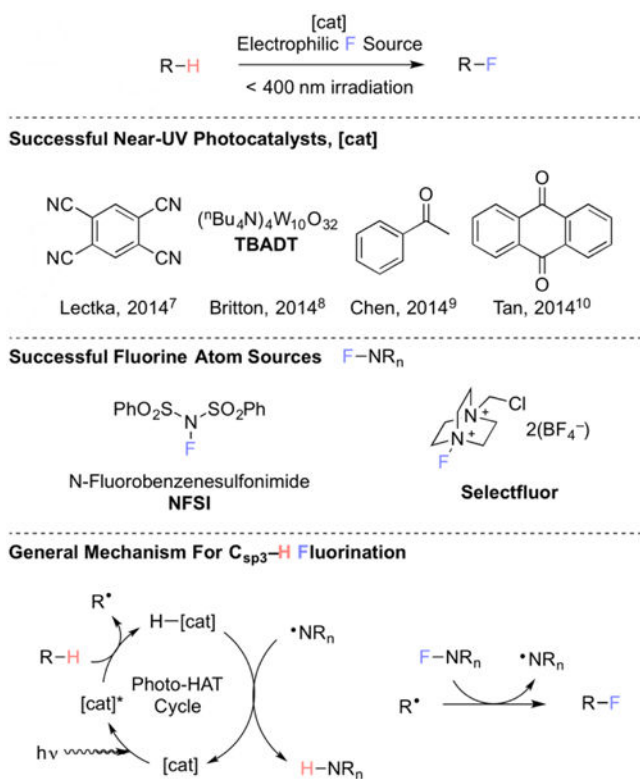


Figure 1. Several near-UV light HAT catalysts and electrophilic fluorine sources used for fluorinations of unactivated C–H bonds and a general mechanism illustrating their function

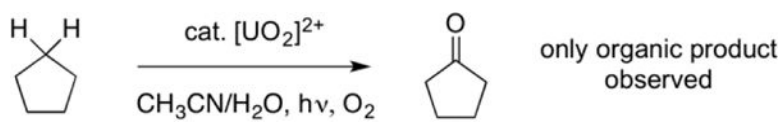


Figure 2. The catalytic aerobic oxidation of alkanes using uranyl cation has been reported

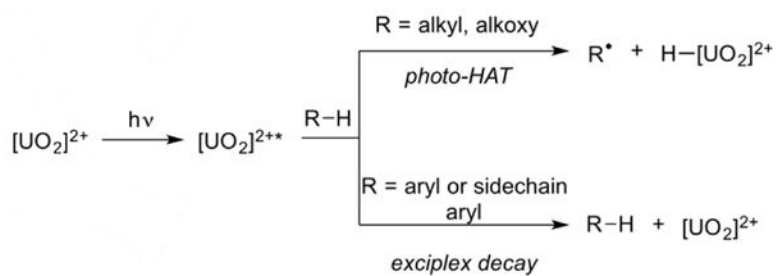


Figure 3. The uranyl excited state $[\text{UO}_2]^{2+*}$ reacts with alkanes primarily through hydrogen atom transfer (HAT) and with arenes through unproductive exciplex decay

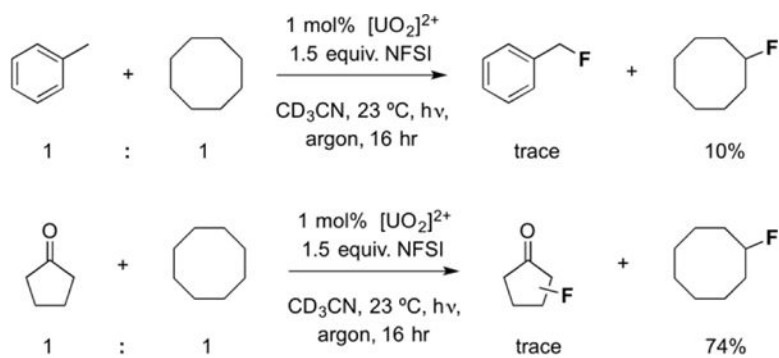
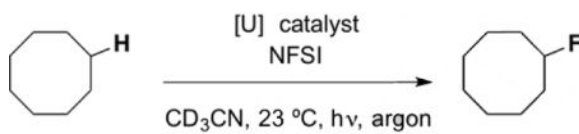


Figure 4. Reactions containing both cyclooctane and toluene (top) or cyclopentanone (bottom) behave differently with respect to reagent conversion. The toluene result suggests that it is an effective quencher of the uranyl excited state $[\text{UO}_2]^{2+*}$.

Table 1

Optimization of cyclooctane fluorination



Entry	NFSI [equiv.]	Catalyst [mol%]	Light Source ^[a]	Yield [%] ^[b]
1	1.5	UO ₂ (OAc) ₂ •4H ₂ O (1)	A	8
2	1.5	UO ₂ (NO ₃) ₂ •6H ₂ O (1)	A	52
3	1.5	UO ₂ (NO ₃) ₂ •6H ₂ O (1)	B	>95
4	1.5	UO ₂ (NO ₃) ₂ •6H ₂ O (1)	none	not observed
5	1.5	none	B	not observed
6	1.2	UO ₂ (NO ₃) ₂ •6H ₂ O (1)	B	73
7	1.5	UO ₂ (NO ₃) ₂ •6H ₂ O (0.5)	B	52
8 ^[c]	1.5	UO ₂ (NO ₃) ₂ •6H ₂ O (1)	B	>95

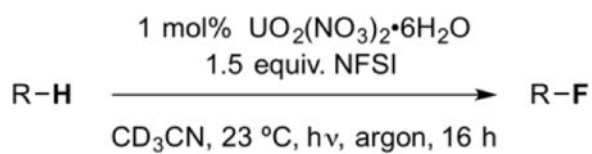
^[a]Light source A: High Density blue LED strip; Light source B: high intensity blue LED lamp

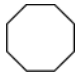
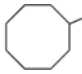

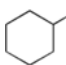

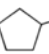

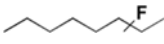

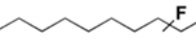
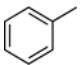
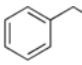
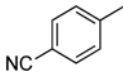
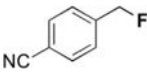
^[b]Yield determined by NMR through integration relative to a methyl acetate internal standard

^[c]Acetone-d₆ used as solvent

Table 2

Fluorination of hydrocarbons

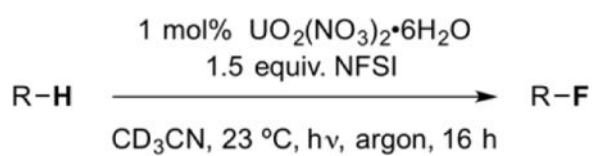



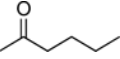
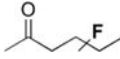
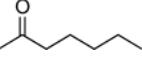
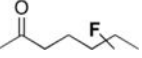
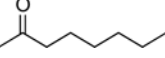
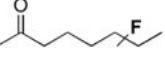
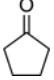
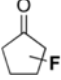
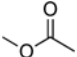
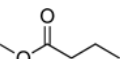
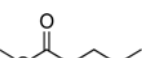
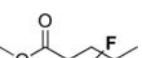




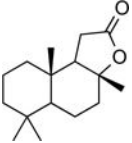
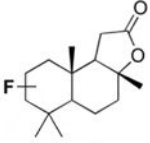

Entry	substrate	product	Yield [%] ^[a]
1			> 95
2			42
3			32
4			55
5			60
6			trace
7			trace

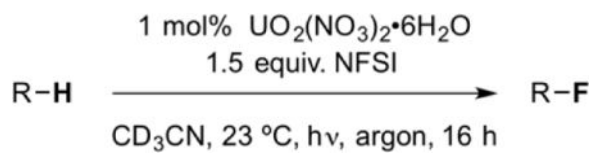
^[a] yield determined by NMR through integration relative to a methyl acetate internal standard

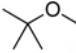
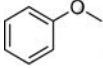
Table 3

Fluorination of Oxygenated Molecules



Entry	substrate	product	Yield [%] ^[a]
1		n/a	No fluorination
2			Trace
3			Trace
4			Trace
5			Trace
6		n/a	No fluorination
7		n/a	No fluorination
8			Trace
9			13
10			10
11			26 ^[b]
12		n/a	No fluorination



Entry	substrate	product	Yield [%] ^[a]
13		n/a	No fluorination
14		n/a	No fluorination

^[a]Yield determined by NMR through integration relative to a methyl acetate internal standard;

^[b]1.6:1 C2/C3 fluorination